Kinetics and Mechanism of Ilmenite Reduction with Carbon Monoxide

Y. Zhao
F. Shadman
Department of Chemical Engineering
University of Arizona
Tucson, AZ 85721

There has been an increasing interest in the reduction of naturally occurring ilmenite. Ilmenite, nominally ferrous metatitanate or $FeTiO_3$, is regarded by manufacturers of titanium dioxide as a raw material alternative to natural rutile. A more recent application is related to material processing in future space stations (Shadman and Zhao, 1989; Briggs and Sacco, 1988). Ilmenite is probably the most important source of recoverable oxygen as well as useful metals on the lunar surface (Cutler and Krag, 1985). A reduction process can be used to produce ultimately gaseous oxygen for fuel and life support.

Most of the available literature describes investigations on naturally occurring ores using carbon, CO or H_2 as reducing agents (Wouterlood, 1979; Poggi et al., 1973; Bardi et al., 1987). From a fundamental point of view, the results of such studies are difficult to interpret because of the complex nature of the ores and the presence of many components. While CO might be an intermediate compound in any carbothermal reduction (Gupta et al., 1987; El-Guindy and Davenport, 1970), the fundamental kinetics and mechanism of ilmenite reduction with CO are not clearly known. Poggi and Charette (1973) studied the reduction of synthetic ilmenite by carbon monoxide. However, their results are difficult to interpret because, under the conditions used in their studies, carbon was also formed from CO disproportionation and participated in the ilmenite reduction.

The purpose of this study is to understand the fundamental mechanism and reaction kinetics of the CO-ilmenite reaction. Carbon monoxide is an important reducing gas because first of all, it is an intermediate product in any carbothermal reduction process. Secondly, CO reduction is potentially an attractive process in which a variety of initial carbonaceous compounds can be used as primary reducing agents for the production of CO.

The kinetics and mechanism of the reduction of synthetic ilmenite were studied in the temperature range of 900 to 1,100°C (which is below the melting point of synthetic ilmenite), with CO concentration of 13% to 23% in a microgravimetric reactor system. The results indicate that the process involves the migration of iron towards the grain boundaries during the reduction, causing separation and segregation of the products: iron and titanium dioxide (rutile) in the grain level. The temporal profiles of conversion indicate the presence of three different stages during the reduction reaction: induction, acceleration, and deceleration.

Experimental Approach

A schematic diagram of the experimental apparatus is shown in Figure 1. The main components of this system are an electronic microbalance (Cahn Instruments, Inc., Model 1000), a quartz flow through reactor with inlet and outlet, and a movable furnace with a PID controller. The composition of gaseous reactants and products was determined using an infrared analyzer and a gas chromatograph. Ilmenite was used in the form of thin flakes pressed from powder. Samples were suspended from the microbalance, which monitored weight changes during the course of an experiment. A thermocouple was used to monitor the temperature of the reactor around the flake. All experiments were performed under isothermal conditions at temperatures between 900 and 1,100°C. The reducing gas entering the reactor contained CO, CO_2 and N_2. The ratio of CO to CO_2 was always maintained at 99 to prevent carbon deposition due to the CO disproportionation reaction (Jones, 1975; Shomate, 1946). The gas flow rate was 260 std. cm^3/min, except in the experiments conducted to determine the effect of interphase mass transfer on the reduction rate.

Samples of starting material were prepared by cold pressing 0.270 g of $FeTiO_3$ powder (with particles size less than 45 μm) in a die of 12.2 mm at 552 MPa for 5 minutes to form disks. The disks were then cut into flakes approximately 10 mm by 8 mm. The thickness of the disks was 0.60 mm except for experiments conducted to determine the effect of intergranular diffusion resistance (transport through void space among grain particles).

Correspondence concerning this paper should be addressed to F. Shadman.

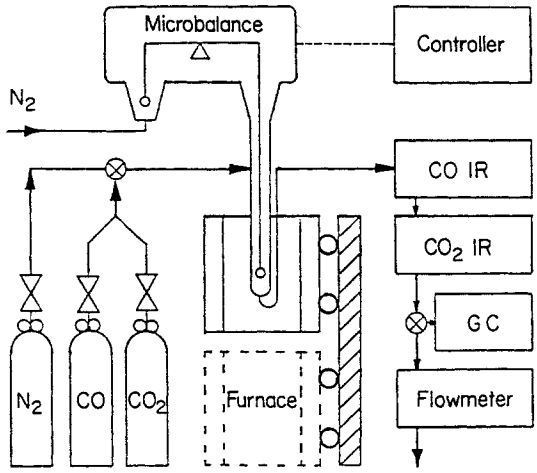

Figure 1. Reactor system.
GC = gas chromatograph
IR = nondispersive infrared analyzer

Each experiment was started by first purging the reactor system at room temperature to reduce the concentration of oxygen to levels below 25 ppm. A mixture of $CO/CO_2/N_2$ was then introduced into the reactor. To initiate the reduction, the furnace was raised rapidly. In less than three minutes, the temperature of the reaction zone was within 1% of the set point temperature. The experiments were terminated at desired conversion by rapidly lowering the furnace.

Several techniques were used for chemical analysis and characterization of the starting and the reduced samples. Mossbauer spectroscopy was employed to determine the oxidation state of iron in our synthetic ilmenite. X-ray diffraction (XRD) with a cobalt Kα source was used to identify the different crystalline phases in the starting material and products. High-resolution scanning electron microscopy (SEM) and energy-dispersive X-ray (EDX) analyses were employed to examine the polished cross section of both partially and completely reduced samples and to determine the elements present in each phase. For SEM and EDX analyses, the samples were mounted in an epoxy resin and polished to expose the cross-section of the grains.

Results and Discussion

The impurity content of our synthetic ilmenite used in this study is given in Table 1. The XRD pattern of our synthetic ilmenite, as shown in Figure 2a, suggests that the sample contains only the $FeTiO_3$ crystalline phase. Mossbauer spectra of the sample show that the synthetic ilmenite used in this study

Table 1. Maximum Impurity Content in the As-Received Synthetic Ilmenite*

Impurity	Max. Conc., wt.%
Al	0.001
Ca	0.01
Cr	0.001
Cu	0.01
MG	0.001
Si	0.1

*CERAC, Inc.

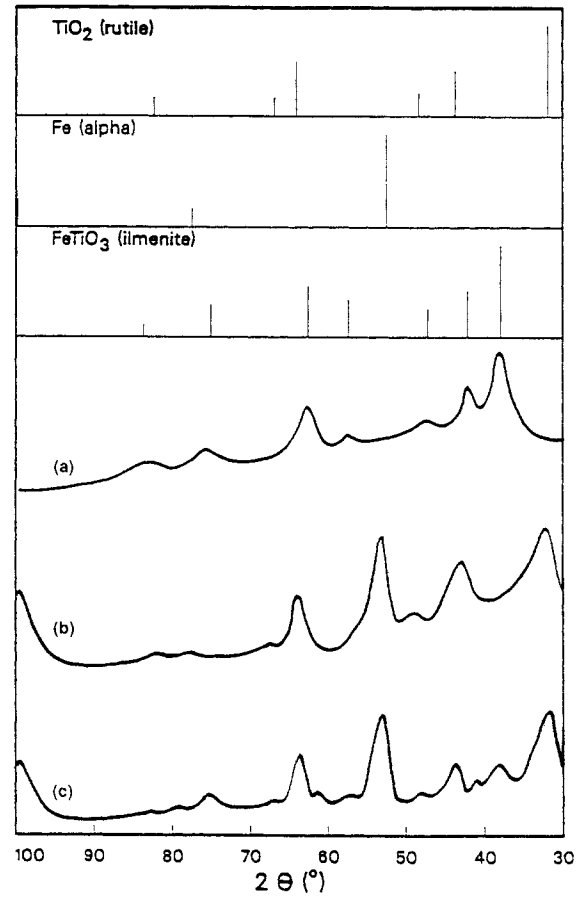

Figure 2. X-ray diffraction spectrum of synthetic ilmenite: a. original pattern; b. after complete reduction at T = 900, 1,000, 1,100°C; c. after partial reduction at T = 1,000°C.

contains only Fe^{++}. This represents the oxidation state of iron in lunar ilmenite.

For each experiment, the sample conversion at any time was determined by two independent methods. The first method was to monitor the sample weight using a recording electrobalance. The second method was to measure the CO_2 generated by the reaction using an on-line infrared gas analyzer. The data from both measurement techniques agreed well with the following stoichiometry:

$$FeTiO_3(s) + CO(g) = CO_2(g) + Fe(s) + TiO_2(s)$$

The first set of experiments were conducted to determine the effect of interphase transport resistance around the flakes. The experiments were conducted at the highest temperature (1,100°C) with 13% CO. It is found that the interphase resistance is not important if the flow rate is at least 260 std. cm^3/min. At temperatures below 1,100°C, the interphase resistance will be even less significant.

The second set of experiments were to determine the effects of intergranular diffusion of CO on the kinetics. These experiments were conducted at the highest temperature (1,100°C) with 23% CO and at a gas flow rate of 260 std. cm^3/min. It is found that the intergranular diffusion of CO does not affect the reduction kinetics if the flake thickness is less than 0.60 mm.

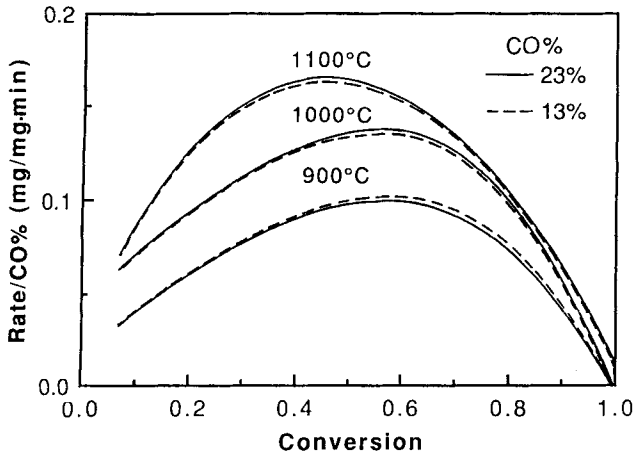

Figure 3. Effect of CO concentration on the reduction rate of ilmenite.

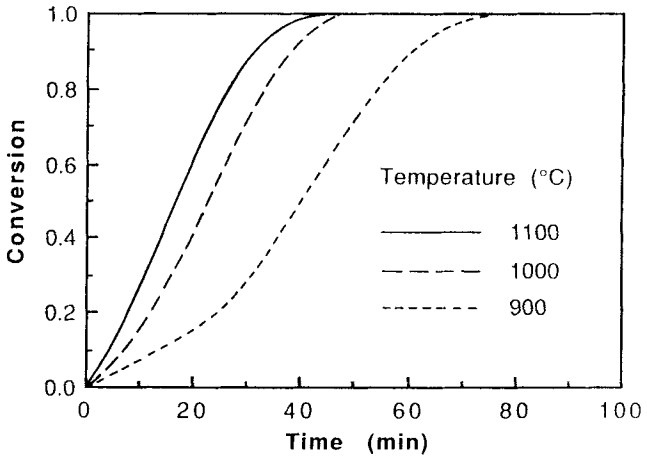

Figure 5. Effect of temperature on the reduction rate of ilmenite: CO% = 23.

To find the reaction order, a series of experiments were conducted at 13% and 23% CO concentration at 900, 1,000, and 1,100°C. The results, shown in Figure 3, show that the reaction order with respect to carbon monoxide is unity in this range of temperature and CO concentration. Therefore, the rate of reaction can be written as

$$r = k(T, X)C_{CO}$$

where rate is expressed in (mg reacted/original mg · min) and C_{CO} in mol/L. k is the apparent rate coefficient and depends on temperature and conversion.

The effect of temperature on the reaction rate at various conversions is shown in Figures 4. The apparent activation energy is 7.5×10^7, 5.9×10^7, and 4.2×10^7 J/kmol at 10%, 30% and 50% conversion level, respectively. As conversion increases, the thickness of the TiO_2 product layer in the grain particles increases. This increases the diffusional resistance against the CO transport into the grain particles. The increase in diffusional resistance causes a decrease in the apparent activation energy.

Isothermal weight loss measurements were performed at 900, 1,000 and 1,100°C. The temporal profiles of conversion at these three temperatures and CO concentration of 23% are shown in Figure 5. These profiles have a sigmoidal shape and indicate the presence of three different stages (induction, acceleration, and deceleration) during the reduction reaction.

To gain insight into the mechanism of the ilmenite reduction, particularly in relation to the observed three stages, samples of both completely and partially reduced ilmenite were analyzed using various analytical techniques. In particular, a combination of optical microscopy, SEM, EDX and XRD analyses provided very useful information on the nature and the distribution of various phases including the products Fe and TiO_2.

A SEM secondary electron micrograph of the polished cross-section of an ilmenite flake after partial reduction at 1,000°C is shown in Figure 6a. The micrograph reveals three distinct regions which appear as bright, light gray and dark gray phases. To identify the phases present, quantitative EDX was

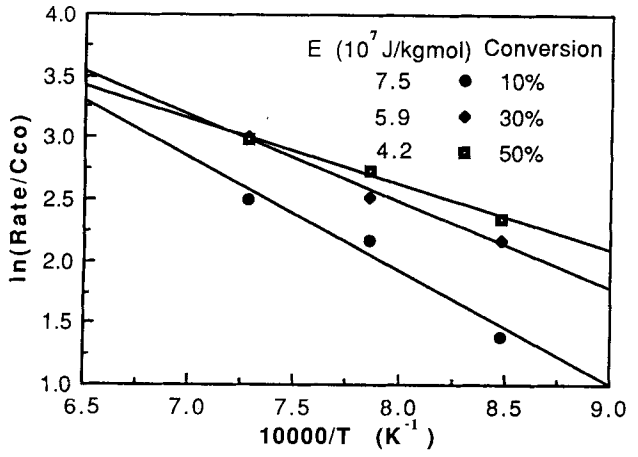

Figure 4. Values of apparent activation energy at 10, 30 and 50% conversion.

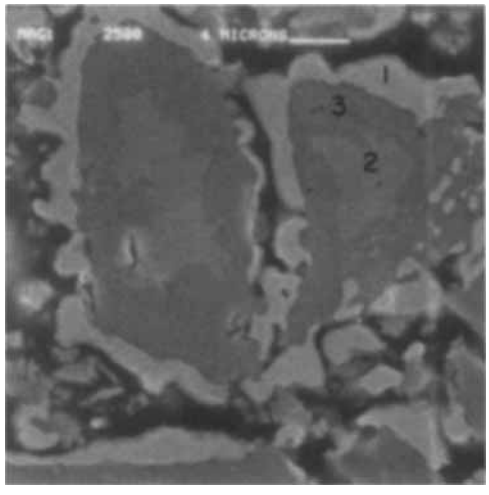

Figure 6a. SEM secondary electron micrograph of the polished cross section of ilmenite flake after partial reduction.

T = 1,000°C, magnification = 2500×
Point 1: 3.1 atom % Ti, 96.9 atom % Fe
Point 2: 51.6 atom % Ti, 48.4 atom % Fe
Point 3: 98.9 atom % Ti, 1.1 atom % Fe

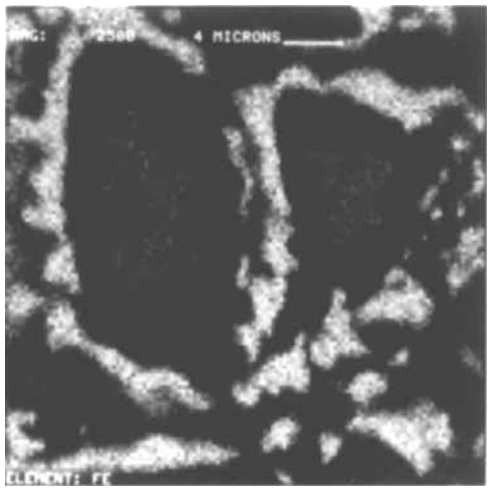

Figure 6b. Fe $K\alpha$ X-ray map of the cross-section shown in 6a.

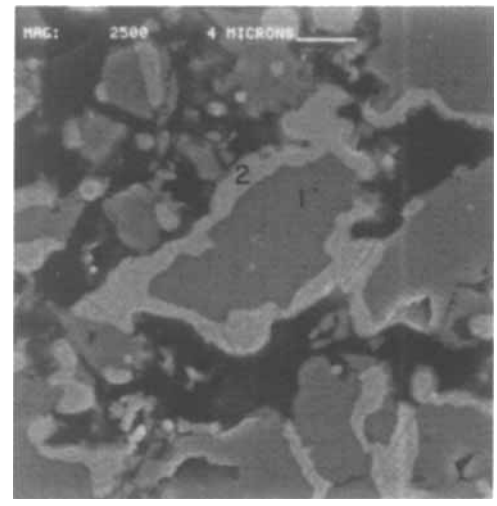

Figure 7a. SEM secondary electron micrograph of the polished cross section of ilmenite flake after complete reduction.

T = 900°C, Magnification = 2500×
Point 1: 99.0 atom % Ti, 1.0 atom % Fe
Point 2: 5.4 atom % Ti, 94.6 atom % Fe

performed at spots marked in Figure 6a. The results and XRD observations (to be discussed later) show that the bright phase is primarily iron, the dark gray phase is made up of titanium dioxide and the light gray phase is unreacted $FeTiO_3$. These results suggest that there is a strong tendency toward the segregation of the products iron and titanium dioxide and that iron diffuses to the grain boundaries through the TiO_2 layer during the reduction. This finding has important implications for product separation and recovery of Fe and TiO_2. Since the reduction temperatures are much lower than the melting point of TiO_2, the TiO_2 product is expected to be in polycrystalline form. As shown in Figure 6a, it appears that the reaction in the grain particles proceeds according to the shrinking core model. This is expected because the grain particles of synthetic ilmenite are nearly nonporous, whereas the product TiO_2 is porous. The corresponding X-ray $K\alpha$ map of iron and titanium, as shown in Figures 6b and 6c, confirm the shrinking core configuration.

The polished cross-sections of synthetic ilmenite flakes after complete reduction at 900 and 1,100°C were also examined by SEM and EDX. The results obtained, as shown in Figures 7 and 8, indicate that a similar mechanism of reduction is involved. However, the coalescence of grains is observed in the flakes reduced at 1,100°C, which is apparently due to the sintering of iron. The EDX analyses of these samples indicate that the phase enriched in titanium is depleted in iron and *vice versa*. This confirms the high degree of segregation of product Fe and TiO_2.

The XRD spectra of both completely and partially reduced samples are shown in Figures 2b and 2c. The phases present after complete reduction at 900, 1,000 and 1,100°C are iron and titanium dioxide; those present after partial reduction at 1,000°C were iron, titanium dioxide, and unreacted ilmenite. These findings confirm the data obtained from EDX analysis.

The various observations described here all point to a mechanism consisting of the following main steps for the reaction in each grain:

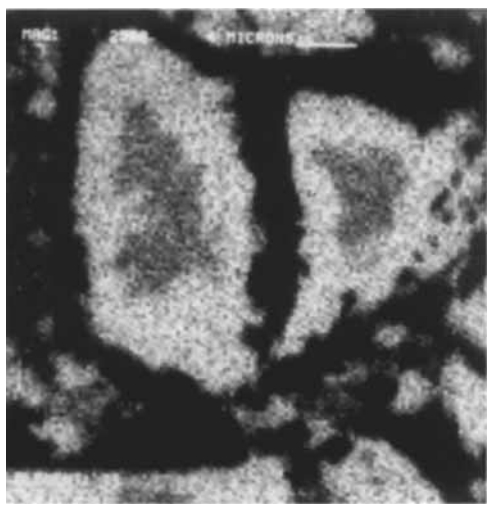

Figure 6c. Ti $K\alpha$ X-ray map of the cross-section shown in 6a.

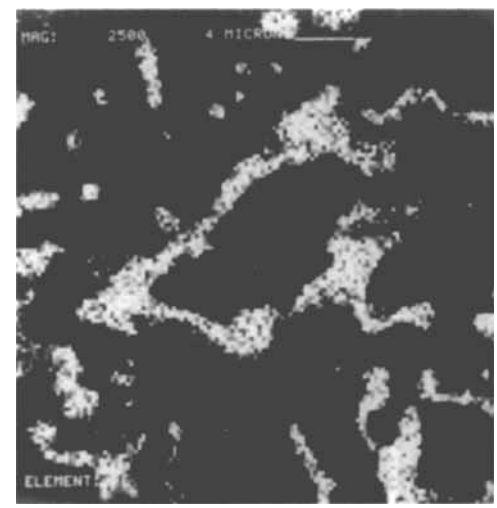

Figure 7b. Fe $K\alpha$ X-ray map of the cross-section shown in 7a.

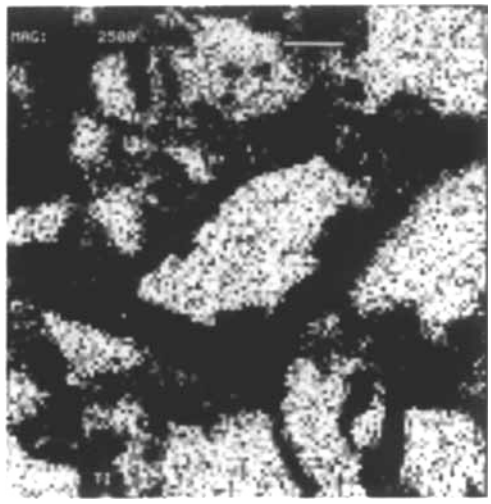

Figure 7c. Ti $K\alpha$ X-ray map of the cross-section shown in 7a.

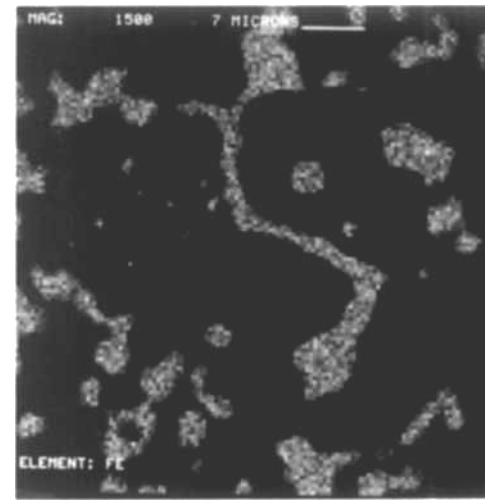

Figure 8b. Fe $K\alpha$ X-ray map of the cross-section shown in 8a.

Step 1. Diffusion of CO through the porous product layer of TiO_2 toward the unreacted core of the grain particles.

Step 2. Reaction of CO with the ilmenite core to produce TiO_2 and Fe.

Step 3. Migration of Fe through the TiO_2 layer away from the unreacted core toward the grain boundary.

Step 4. Formation of iron nuclei and their subsequent growth outside and around the reacted grain particles.

Steps 3 and 4 result in almost complete segregation of the two solid products, iron and titanium dioxide, in the scale of grains.

An important point concerns the driving force behind the migration of iron followed by its nucleation and growth around the grain particles. Iron produced during the reduction reaction is distributed in the pores of titanium dioxide and has a higher activity than the agglomerated pure iron mass growing outside the grain particles. This is due to the fact that the small iron islands on the surface are less stable and move toward a large iron mass to agglomerate. Thermodynamically, this is in the direction of minimizing the total surface energy.

Using the proposed mechanism, the three stages observed during conversion can be described as follows:

Induction Stage. This represents the initial stage of the reduction process when the reaction is relatively slow. The induction period is definitely a genuine property of the reaction mechanism and is not due to a delay in heating up the sample which is relatively short. Moreover, the duration of the induction period decreases as the set point reaction temperature increases (15 minutes at 900°C and 5 minutes at 1,100°C). This is the opposite of the trend expected for any possible effect of transient reactor heat-up.

A possible mechanism for the observed induction stage is the delay in the nucleation and growth of iron phase. Initially, the iron produced by the reaction accumulates in the porous structure of the TiO_2 product layer. In this stage, the rate of iron production is faster than the rate of iron transport out of the

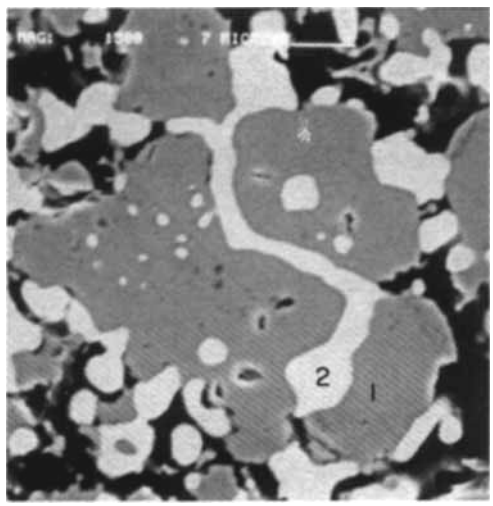

Figure 8a. SEM secondary electron micrograph of the polished cross section of ilmenite flake after complete reduction.

T = 1,100°C, magnification = 2500×
Point 1: 99.0 atom % Ti, 1.0 atom % Fe
Point 2: 2.5 atom % Ti, 97.5 atom % Fe

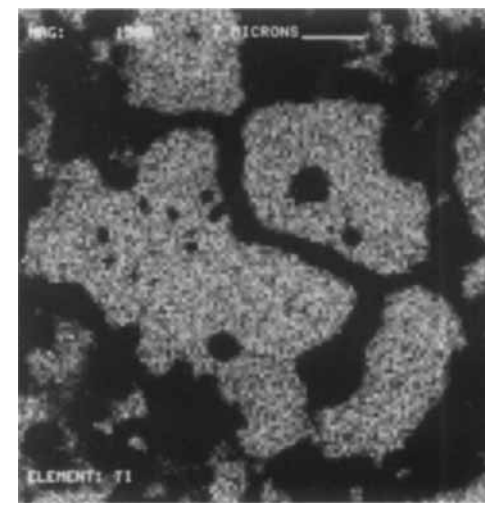

Figure 8c. Ti $K\alpha$ X-ray map of the cross-section shown in 8a.

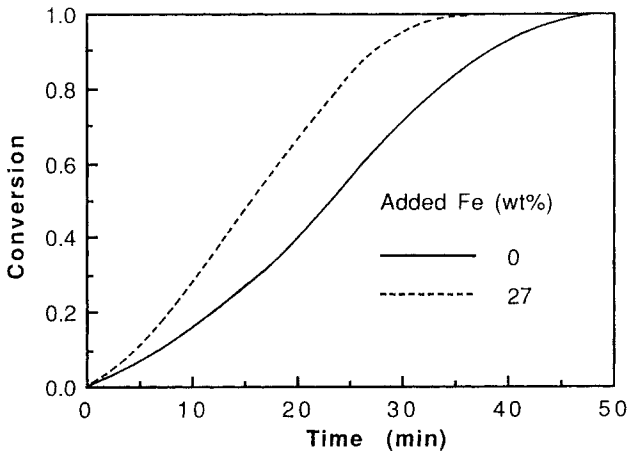

Figure 9. Effect of iron addition on the reduction rate of ilmenite: CO% = 23, T = 1,000°C.

TiO_2 layer. Consequently, TiO_2 pores are partially plugged and CO access to the reaction front is restricted.

Acceleration Stage. As reaction goes on, more iron is produced and transported to the grain boundaries, forming new nuclei and increasing the growth rate of iron phase. This facilitates the transport of iron and opens up the TiO_2 pores. Consequently, CO transport to the reaction front is enhanced and a significant increase in the reaction rate is observed. It is important to note that the rapid rise in rate during the second stage is not due to any autocatalytic effect of iron accumulation. The nucleation and accumulation of iron is outside the grain particles and not on the reaction surface. The accumulated iron and the reaction interphase are separated by a layer of nonreactive titanium dioxide.

Deceleration Stage. Finally, depletion of $FeTiO_3$ results in a decrease in the rate of reduction.

For a direct observation of the effect of iron nucleation on the rate in a series of experiments, a known amount of iron powder with the particle size less than 45 μm was added to ilmenite powder before pressing. As shown in Figure 9, the addition of iron reduces the length of the induction period significantly. This confirms the suggestion that the low rate during the initial induction period is due to the absence of sufficient iron nuclei. This causes slow transport of iron away from the reaction front and inhibition of CO contact with the unreacted $FeTiO_3$. As stated before, the observed effect of iron addition or accumulation is not catalytic because the added or the accumulated iron phase is separated from the reaction surface by a layer of titanium dioxide.

Acknowledgment

This research was supported by NASA/UA Center for Utilization of Local Planetary Resources at the University of Arizona. Mr. G. Chandler provided invaluable technical assistance in SEM and EDX analyses. X-ray spectra were performed by Dr. L. J. Demer. Discussions with Dr. A. Cutler, Mr. E. A. Bassham, and Mr. M. Uberoi have been very helpful in this study.

Notation

C_{co} = CO concentration, mol/L
k = apparent rate coefficient, mg reacted · L/original mg · min · mol
E = apparent activation energy, J/kmol
r = reaction rate, mg reacted/original mg · min
X = conversion of $FeTiO_3$
T = temperature

Literature Cited

Bardi, G., D. Gozzi, and S. Stranges, "High Temperature Reduction Kinetics of Ilmenite by Hydrogen," *Mat. Chem. and Phys.*, **17**, 32 (1987).

Briggs, R. A., and J. A. Sacco, "Oxidation and Reduction of Ilmenite: Application to Oxygen Production on the Moon," *Symp. NASA*, Houston, paper No. LBS-88-170 (1988).

Cutler, A. H., and P. Krag, "A Carbothermal Scheme for Lunar Oxygen Production," *Lunar Bases and Space Activities in the 21st Century*, ed., W. Mendell (1985).

El-Guindy, M. I., and W. G. Davenport, "Kinetics and Mechanism of Ilmenite Reduction with Graphite," *Metal. Trans.*, **1**, 1729 (1970).

Gupta, S. K., V. Rajakumar, and P. Grieveson, "Kinetics of Reduction of Ilmenite with Graphite at 1,000 to 1,100°C," *Metal. Trans.*, **18B**, 713 (1987).

Jones, D. G., "Kinetics of Gaseous Reduction of Ilmenite," *J. Appl. Chem. Biotechnol.*, **25**, 561 (1975).

Poggi, D., G. G. Charette, and M. Rigaud, "Reduction of Ilmenite and Ilmenite Ores," *Titanium Science and Technology*, **1**, 247, eds., R. I. Jaffee and H. M. Burte, Plenum Publishing (1973).

Shadman, F., and Y. Zhao, "Production of Oxygen from Lunar Ilmenite," Annual Progress Report, NASA/UA Center for Utilization of Local Planetary Resources, I-1 (1988–1989).

Shomate, C. H., B. F. Naylor, and F. S. Boericke, U.S. Bur. Mines Rep. of Invest. No. 3864 (1946).

Wouterlood, H. J., "The Reduction of Ilmenite with Carbon," *J. Chem. Tech. Biotechnol.*, **29**, 603 (1979).

Manuscript received Feb. 5, 1990, and revision received June 15, 1990.